JOURNAL OF PROPULSION AND POWER
Vol. 25, No. 6, November–December 2009

Simulation of Supersonic Combustion in Three-Dimensional Configurations

P. G. Keistler* and H. A. Hassan†
North Carolina State University, Raleigh, North Carolina, 27695-7910
and
X. Xiao‡
Corvid Technologies, Mooresville, North Carolina, 28117

DOI: 10.2514/1.43848

A turbulence model that calculates the turbulent Prandtl and Schmidt numbers as part of the solution, addresses turbulence/chemistry interactions, and accounts for compressibility effects is used to simulate supersonic combustion in two three-dimensional experiments: the SCHOLAR experiment, which employs vitiated air and hydrogen fuel, and the HyShot experiment, which employs air and hydrogen fuel. Two chemical kinetic models are employed: one employs reaction rates that are functions of temperature, whereas the other employs rates that are both functions of pressure and temperature. In general, fair to good agreement is indicated with available measurements.

I. Introduction

SIMULATION of turbulent combustion in scramjet engines requires highly sophisticated models to address the complex flow physics involved. Earlier work [1] using turbulence models that only consider velocity fluctuations, such as k-ε or k-ω models, demonstrated the profound influence of the turbulent Prandtl number Pr_t, and turbulent Schmidt number Sc_t, on the simulation. Thus, low values of Sc_t can enhance mass transfer and subsequent heat release to such an extent that they may result in unstarts. On the other hand, high values of Sc_t will result in the reduction of turbulent mass transfer to levels that could not sustain combustion. Similarly, reduced values of Pr_t result in increased thermal diffusion away from the flame holding, with the result that flame blowout may occur.

When dealing with reacting high-speed flows, concentrations and temperature fluctuations are as important as velocity fluctuations. Thus, to asses the role of such fluctuations on supersonic combustion, equations for the variance and dissipation rate of enthalpy and concentrations are required. Rather than rely on equations suited for low-speed flow or empirical formulations, required equations were derived from the exact compressible Navier–Stokes equations and were modeled term by term. The approach employed followed procedures established in the k-ζ turbulence closure model [2]. Thus, the complete set consists of six equations: turbulence kinetic energy or variance of velocity k, variance of vorticity or enstrophy ζ, variance of enthalpy $\tilde{h}''^2$, and its dissipation rate ε_h, variance of concentrations σ, and its dissipation rate ε_Y. The resulting set of equations is tensorially consistent, Galilean invariant, coordinate-system independent, and is free of wall or damping functions.

Compressibility at high Mach numbers limits the spreading rate of injected fuel and has a significant influence on mixing of fuel and oxidizer. The model of [3] was used. This model was validated by three sets of supersonic mixing experiments [4–6], in which detailed measurements of velocity profiles, turbulent kinetic energy, and turbulent stresses were presented.

Turbulence/Chemistry interaction plays a major role in supersonic combustion. The traditional manner in which such interactions are addressed is through the use of assumed and/or evolution probability density functions (PDFs). Calculations employing both approaches were compared in [7] for supersonic combustion of parallel streams. It was shown there that both formulations yield comparable mean flow. However, assumed PDFs were unable to predict higher order correlations, such as those involving chemical source terms, with any reasonable accuracy. Computations employing evolution PDFs are time consuming and require excessive storage because the solution is carried out using a Monte Carlo method. Because of this, all higher order correlations involving chemical production terms were modeled in [8].

The present work employs the model of [8], which presents the detailed set of model equations and validations using 2-D/axisymmetric experiments involving mixing and combustion. The next step of the validations process is to apply the model of [8] to 3-D supersonic combustion experiments that exhibit some of the geometric complexities of proposed scramjet designs. One such experiment is referred to as the SCHOLAR experiment [9,10]. This experiment, which was conducted at the NASA Langley Research Center Direct-Connect Supersonic Combustion test facility, is one of the experiments adopted by a working group of the NATO Research and Technology Organization as a test case for CFD development and validation activity.

The model design of the experiment was based on a simulation using the viscous upwind algorithm for complex flow analysis (VULCAN) code [11] with emphasis on avoiding large regions of subsonic recirculating flows. It became evident later that the design resulted in a situation in which chemical reactions greatly lagged mixing with the result that combustion took place downstream of the hydrogen injector.

A CFD simulation of the SCHOLAR experiment was carried out by a number of authors [12,13] using the VULCAN code. This code has no provisions for calculating the turbulent Schmidt and Prandtl numbers as part of the solution but has limited capability in addressing chemistry/turbulent interactions using assumed PDFs. A rather detailed sensitivity study of the various parameters that could conceivably affect the flow in the combustor was undertaken. It was concluded that the solution was greatly effected by the selection of the turbulent Prandtl and Schmidt numbers and the turbulence and chemical kinetic models. In spite of this exhaustive study none of the parameters considered resulted in the prediction of the correct ignition location.

Received 17 Feb. 2009; revision received 12 Aug. 2009; accepted for publication 18 Aug 2009.

*Graduate Student, Mechanical and Aerospace Engineering Department. Student Member AIAA.
†Professor, Mechanical and Aerospace Engineering Department. Fellow AIAA.
‡Senior Aerospace Engineer.

The second experiment was performed by researchers in the HyShot program at the University of Queensland (Australia) [14]. This experiment consists of a complete scramjet engine model. One purpose of these experiments, other than demonstrating sustained scramjet operation, was not to produce optimal thrust but rather to examine the effects of combustor height, equivalence ratio, and freestream enthalpy on ignition and steady operation of the scramjet engine. Another purpose of the experiment was to test the concept of the radical-farm ignition process in which combustion induced pressure rise takes place in subsequent hot pockets rather than in the first.

A simulation of the HyShot experiment was performed by Star et al. [15] using various combinations of constant turbulent Prandtl and Schmidt numbers. The best results were obtained with a Pr_t of 0.9 and Sc_t of 0.5, but the downstream pressure was still overpredicted by the model.

The work of Mattick et al. [16] employs variable turbulent Prandtl and Schmidt numbers formulation and allows for compressibility effects but not turbulence/chemistry interaction. The variable turbulent number formulation is based on the incompressible energy equation. On the other hand, the variable Schmidt number formulation is based on a mixture fraction variance equation. The two sets of equations for the turbulent Prandtl and Schmidt numbers are formally similar and employ the same set of model constants.

One of the configurations selected for this investigation employed vitiated air whereas the other employed dry air. The effect of vitiated air was discussed by Tomioka et al. [17]. They indicated that matching the flow total enthalpy essentially eliminated the effects of other flow conditions on engine performance.

A number of computational efforts that used a variety of turbulence models in which both the turbulent Prandtl and Schmidt numbers were assumed constant were undertaken. Lee [18] simulated the mixing characteristics of dual transverse injection in a scramjet combustor using the k-ω shear stress transport model. He showed that dual injection results in higher mixing and penetration than single injection. However, it results in greater stagnation pressure loss. The same conclusion was arrived at in the presence of combustion [19]. Unfortunately, no comparison with experiment was presented. Another computational study of the propulsive characteristics of a shock induced combustion ramjet was conducted by Alexander and Sislian [20]. The k-ω model was employed and again, no comparison with experiment was presented.

A 2-D numerical study of supersonic combustion was undertaken by McGuire et al. [21] to investigate the radical-farm ignition system. They showed that, for the premixed 2-D configuration considered, the first hot spot acted like a radical farm.

The SCHOLAR experiment was the subject of investigation by the current authors [22–24] with limited success. It became evident after thorough investigation that numerical and coding errors were made in previous investigations. These errors were not related to the model or the results of [8]. These are corrected in the present investigation.

II. Formulation of the Problem

A. Governing Equations

The details of the model are presented in [8]. Because of this, only a brief summary is presented here. The variable Pr_t and Sc_t formulations employed in this work are based on equations for the variance and dissipation rate of enthalpy and the variance and dissipation rate of concentrations. The variance of enthalpy $\tilde{h}''^2$ and its dissipation rate ε_h provide an expression for α_t the turbulent diffusivity in the form

$$\alpha_t = 0.5(C_h k\tau_h + \nu_t/\beta_h) \tag{1}$$

where

$$\tau_h = \widetilde{h''^2}/\varepsilon_h, \qquad \varepsilon_h = \alpha\overline{\left(\frac{\partial h''}{\partial x_i}\right)^2} \tag{2}$$

ν_t is the turbulent eddy viscosity,

$$\nu_t = C_\mu k^2/\nu\zeta, \qquad C_\mu = 0.09 \tag{3}$$

C_h is a model constant, α is the laminar diffusivity, and ν is the molecular kinematic viscosity. The parameter β_h is chosen here as 0.5. The turbulent Prandtl number Pr_t is given by

$$Pr_t = \nu_t/\alpha_t \tag{4}$$

Similarly, the variance of concentrations σ_Y

$$\sigma_Y = \sum \widetilde{Y_m''^2} \tag{5}$$

in which Y_m'' is the fluctuation of the mass fraction of species m and its dissipation rate ε_Y

$$\varepsilon_Y = \sum \overline{D\left(\frac{\partial Y_m''}{\partial x_i}\right)^2} \tag{6}$$

yields the turbulent diffusion coefficient D_t as

$$D_t = 0.5(C_Y k\tau_Y + \nu_t/\beta_Y) \tag{7}$$

where

$$\tau_Y = \sigma_Y/\varepsilon_Y \tag{8}$$

C_Y and β_Y are model constants and D is the molecular binary diffusion coefficient. The turbulent Schmidt number Sc_t is defined as

$$Sc_t = \nu_t/D_t \tag{9}$$

It should be noted that both Pr_t and Sc_t are calculated after convergence is achieved.

The equation for σ_Y, the variance of concentrations, contains the term

$$\sum \overline{Y_m''\dot{\omega}_m}$$

in which $\dot{\omega}_m$ is the production rate of species m. Similarly, the equation that governs the enthalpy variance contains the term

$$\sum \overline{h''\dot{\omega}_m \Delta h_{f,m}}$$

in which $\Delta h_{f,m}$ is the heat of formation of species m. Traditionally, the preceding terms are evaluated by using assumed or evolution PDFs, or ignored completely. Because such terms are important, a modeling approach was implemented in [8]. Thus,

$$2\sum \overline{Y_m''\dot{\omega}_m} = C_{Y,8} \sum \sqrt{\widetilde{Y_m''^2}}\,\bar{\dot{\omega}}_m \tag{10}$$

and

$$\sum \overline{h''\dot{\omega}_m \Delta h_{f,m}} = C_{h,12}\sqrt{\widetilde{h''^2}} \sum \overline{\dot{\omega}_m \Delta h_{f,m}} \tag{11}$$

in which $C_{Y,8}$ and $C_{h,12}$ are model constants and $\bar{\dot{\omega}}_m$ is the value of $\dot{\omega}_m$ using mean temperature and mass fractions. Because evolution PDF methods are computationally intensive requiring extensive computer time and excessive storage, the preceding modeling results in a highly efficient algorithm.

The compressibility correction results from the dilatational dissipation term

$$\frac{4}{3}\nu\overline{\rho(u_{i,i}'')^2}$$

and a pressure work term

$$\overline{u_i''}\frac{\partial P}{\partial x_i}$$

that appear in the k equation. Typical models assume the dilatational dissipation term to be proportional to $M_t \sim k/a^2$ the turbulent Mach number. On the other hand, the k-ζ model models the term as [2]

$$\frac{4}{3}\nu\overline{\rho(u''_{i,i})^2} = C_1\bar{\rho}k/\tau_\rho, \qquad C_1 = 0.6 \tag{12}$$

where

$$\frac{1}{\tau_\rho} = \frac{1}{\bar{\rho}}\left[k\left(\frac{\partial\bar{\rho}}{\partial x_i}\right)^2\right]^{\frac{1}{2}} \tag{13}$$

The pressure work term is modeled as

$$\overline{u''_i}\frac{\partial P}{\partial x_i} = \frac{\nu_t}{C_k\bar{\rho}}\frac{\partial\bar{\rho}}{\partial x_i}\frac{\partial P}{\partial x_i} \tag{14}$$

B. Numerical Procedure

A modification of REACTMB [25], a code that has been under development at North Carolina State University for the last several years, is employed in this investigation. It is a general purpose parallel Navier–Stokes solver for multicomponent multiphase reactive flows at all speeds. It employs a second order essentially nonoscillatory and/or total variation diminishing upwind method based on the low-diffusion flux-splitting scheme of Edwards [26] to discretize the inviscid fluxes, whereas central differences are employed for the viscous and diffusion terms. Plane relaxation is employed. A simplified version in which the species and conservation equations are decoupled from the turbulence equations is employed for the 3-D calculation. This results in a more efficient algorithm and is recommended when the computer resources are limited. Comparison of the two approaches showed that both gave the same results. The code is parallelized using domain decomposition and message passing interface strategies.

Methods that employ plane relaxation require the inversion of large matrices. Based on experience with the 3-D calculations, the matrix inversion has to be carried out for each iteration and the CFL number is limited to 1; otherwise inaccurate results may be obtained.

C. Chemical Kinetic Models

Two completely distinct H_2/air mechanisms were considered in [8]. The first is the seven species/seven reactions model developed by Jachimowski [27]. In this mechanism, the seven species considered are H_2, O_2, OH, H_2O, H, and O, together with the inert species N_2. In addition, all reaction rates are functions of temperature. The second is the nine species/nineteen reaction mechanism developed by Connaire et al. [28]. This model considers all of the preceding species as well as HO_2 and H_2O_2. Moreover, the reaction rates are both pressure and temperature dependent. This model was developed for combustion over a temperature range of 298–2700 K, a pressure range of 0.01–87 atmospheres, and equivalence ratios from 0.2–6. It has been shown in [8] that both of the preceding chemical mechanisms produce the same results. Therefore, only the Jachimowski mechanism is employed in the results presented here.

D. Description of the Experiments

A schematic of the SCHOLAR experiment is shown in Fig. 1. It consists of two main sections of duct: a copper upstream section, and a carbon steel downstream section. As is seen from the figure there is a constant area segment, a small outward step at the top wall, and a second constant area segment followed by a segment with constant 3 deg divergence at the top wall. The main fuel injector is located just downstream of the 3 deg divergence. The injector angle is 30 deg to the opposite wall. The injector nozzle is designed to produce Mach 2.5 flow at injector exit. The experiment was conducted at the NASA Langley Direct-Connect Supersonic Combustion Test Facility. Vitiated air, which results from hydrogen burning in oxygen-enriched

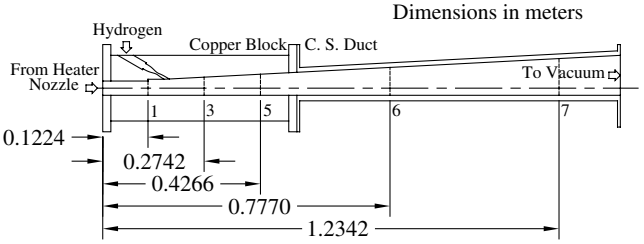

Fig. 1 Schematic of SCHOLAR experiment.

air, is accelerated through a water-cooled converging-diverging Mach 2 nozzle before entering the test model. The test conditions are nominally representative of Mach 7 flow. Gas flow rates to the heater are 0.915 ± 0.008 kg/s air, 0.0284 ± 0.0006 kg/s H2, and 0.300 ± 0.005 kg/s O2. The heater stagnation pressure is 0.765 ± 0.008 MPa and the stagnation temperature is 1827 ± 75 K. The composition leaving the heater is determined from a one-dimensional analysis. Uncertainties due to random run–to–run variations were estimated to be 95%. These uncertainties do not include the $\pm 3\%$ uncertainty in the mass flow rate measurements.

Hydrogen is injected at a stagnation pressure of 3.44 ± 0.065 MPa and a stagnation temperature of 302 ± 4 K. The H2 flow rate corresponds to an overall equivalence ratio of 0.99 ± 0.04 for the gas in the duct. The main duct is uncooled. This limited the run times to about 20 s without reaching excessive wall temperatures. Further, the duct has seven slots to allow measurements of temperature and composition by Coherent anti-Stokes Raman Spectroscopy (CARS). As is seen from Fig. 1, the first slot is at the main nozzle exit and the other six are downstream of the fuel injection nozzle. The slots are 4.8 mm wide and extend the full height of the duct. Measurements were carried out at slots 1, 3, 5, 6, and 7. Further details are available in Refs. [9,10].

A schematic of the HyShot experiment is shown in Fig. 2. This experiment consists of a complete scramjet engine model. As mentioned earlier, the purpose of these experiments, other than demonstrating sustained scramjet operation, was not to produce optimal thrust, but rather to examine the effects of combustor height, equivalence ratio, and freestream enthalpy on ignition and steady operation of the scramjet engine. The overall design was driven by attempting to minimize drag, which lead to flush wall fuel injectors, the absence of mixing enhancement devices, and an inlet designed with two mild compressions rather than one. The fuel injectors were placed on the inlet ramp in an attempt to compensate for the lack of these mixing mechanisms. The side walls of the model in the inlet section are cut away in a V shape to reduce boundary-layer growth and allow the model to be self starting.

The total length of the model is 0.625 m and the width is 0.075 m. There are a total of eight sonic fuel injectors on the inlet surface, four on the top and four on the bottom ramp. These injectors are equally spaced between the side walls and angled 45 deg with respect to the inlet surface. The inlet surfaces are inclined at 9- and 12 deg, whereas the nozzle is a constant 9 deg expansion. The combustor height for the particular case presented, number 7678, is 24 mm. The freestream Mach number in the shock tunnel is 6.42, with a static pressure of 8958 Pa and a static temperature of 412 K. The stagnation pressure and temperature of the fuel injectors are 1.22 MPa and 300 K, respectively. The equivalence ratio for these conditions is 0.51. The experimental data consist of pressure measurements along the center of the bottom wall during the steady portion of the operation.

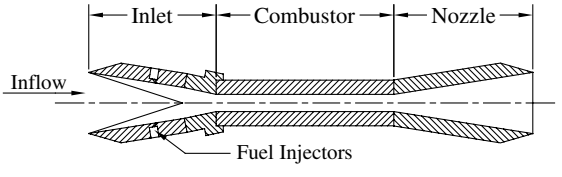

Fig. 2 Schematic of HyShot engine model.

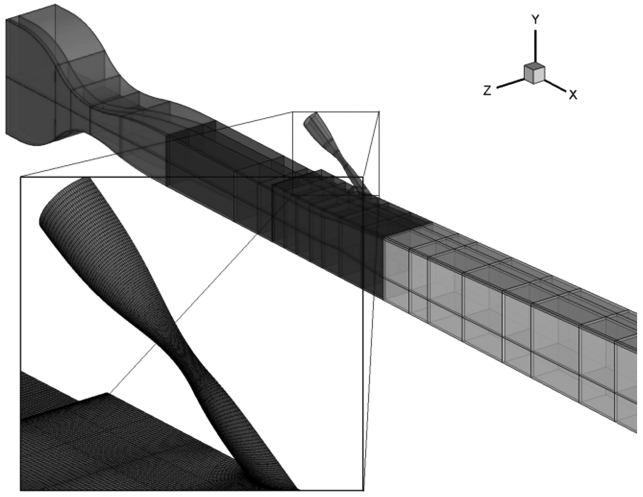

Fig. 3 Computational grid for SCHOLAR case with detail of hydrogen injector.

III. Results and Discussion

A. SCHOLAR Experiment

Calculations were carried out throughout the device using input plenum conditions for the main and hydrogen nozzle. The configuration of the device showing the block structure used in the computation is shown in Fig. 3. The computation employed 378 blocks and 50 processors. Two grids, each containing 7,522,835 grid points were employed in this study; they differ in that one clusters more points along the shear layer resulting from mixing of H_2 and vitiated air.

Because no wall cooling was employed, tests were run for 20 sec and were resumed after the duct cools. It took one day to complete the measurements on each of the first four planes (1, 3, 5, 6) and two days on plane 7. Static pressure taps were located on the centerline of the bottom wall, on the top wall (close to the sidewall of the copper section and centerline of the steel section), and midpoints of the sidewall of the steel section. Thermocouples were located at the top wall. Because the duct was not cooled, the wall temperature varied greatly over a 20 sec run. It ranged from 320–500 K for the copper and 320–890 K for the steel section. The present calculation assumed that the temperature in the ghost cell next to the wall to be 475 K for the copper and 600 K for the steel section. It should be noted that results of [13] showed that wall temperature has little influence on calculated results.

The computed and measured pressure distributions along the bottom wall are shown in Fig. 4. Whereas there are some obvious excessive shock reflections in the region from $x = 0.4$ to $x = 0.6$ m, the overall pressure distribution is matched quite well, especially in the downstream section. Figure 5 shows the computed and measured temperature distributions on the CARS measurement planes. The computed data are on the left half of each plane, and the experimental surface fits are on the right side of each plane. There is fair agreement overall, but early ignition is indicated on the third plane. Note that the method of generating the surface fit may eliminate sharp features such as those seen in the computed contours. Regardless of this fact, early ignition could be an issue not only with the model but also the grid, the chemical model, the time-advancement scheme, etc. Species mole fraction contours for both nitrogen and oxygen are shown in Fig. 6. Again, the computed distribution is a fair match to the experimental surface fits.

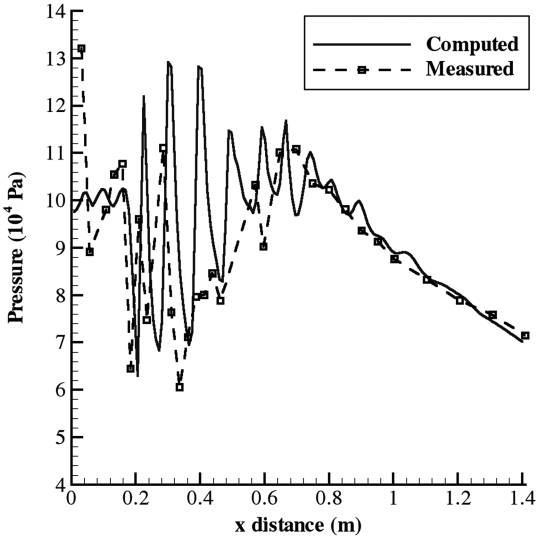

Fig. 4 Pressure distribution along center of bottom wall.

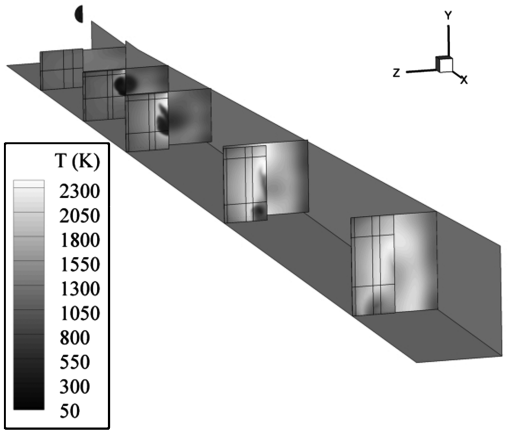

Fig. 5 Temperature distribution on CARS measurement planes: computed data on left, experimental data on right of each slice.

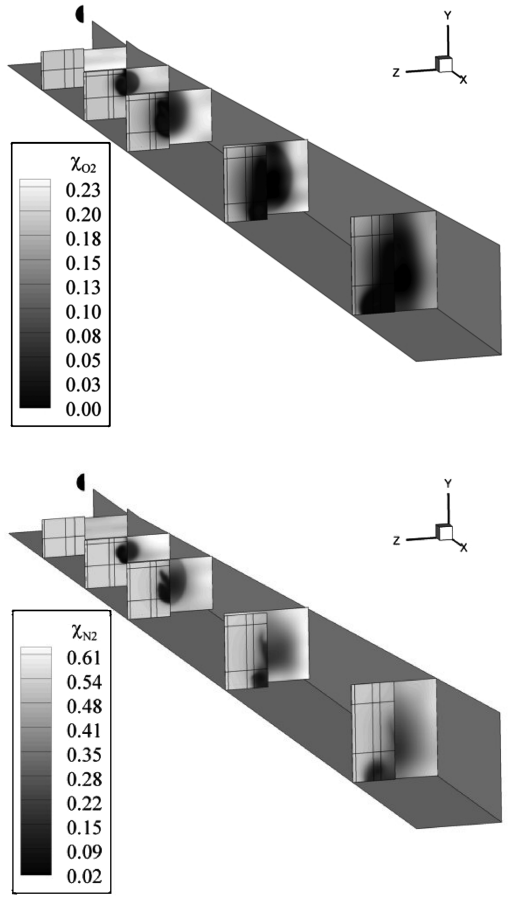

Fig. 6 Mole fraction distributions: oxygen (top), and nitrogen (bottom).

The computed turbulent Prandtl and Schmidt numbers can be seen in Fig. 7. The Prandtl number reaches the floor value of 0.2 throughout the mixing and combustion region. This behavior has been observed for the present model previously in cases involving combustion [19]. The Schmidt number behaves in a similar manner but starts to recover toward the end of the duct, again consistent with previous findings. Note that the floor value for the Schmidt number in this case is 0.33. The indicated behavior of the turbulent Schmidt and Prandtl numbers is a result of intense fluctuations of concentrations in the presence of mixing and combustion. This is reflected in the definitions of D_t and α_t. Reduced Sc_t and Pr_t result in enhanced mass transfer and thermal diffusion away from the flame. It appears that the current model provides the needed balance that resulted in fair agreement with experiment.

B. HyShot Experiment

The grid used for the HyShot case employs 400 blocks and 5.43 10^6 cells. This is the same grid used in [15] but decomposed into more blocks. The grid makes use of the bilateral symmetry of the experimental model so that the computational model is only one quarter actual domain. A spillage region is included adjacent to the sidewall cutouts. Note that the side walls in the computational model are infinitely thin, and the boundary conditions are modified between the inlet blocks and the spillage blocks to account for the cutout. Also, rather than modeling the hydrogen injectors exactly, a different boundary condition is employed on the wall over the region in which each injector would be, imposing a uniform sonic fuel injection profile.

The results presented here are for run number 7678 which resulted in stable combustion. A time-accurate calculation of this case was carried out in [15]. It was pointed out there that the results were sensitive to the manner in which wall temperature is specified. The best results were obtained by coupling the time-dependant heat conduction equation to the time-dependant flow solver. Because the experiment resulted in steady combustion, a steady calculation is carried out here. In the present calculations, the ghost cell in the wall is assumed to have a value equal to that of the ambient temperature.

The computed and measured pressure distributions are shown in Fig. 8. The agreement is good through the inlet and first half of the combustor, but from approximately $x = 0.3$ m to the exit of the engine the predicted pressure is lower than the measured pressures. The discrepancy is most likely due to the lack of fuel combustion in the center of the model. The outer fuel jet ignites in the first half of the combustor and the flame persists through to the exit of the nozzle, but the inner fuel jet does not ignite. This can be seen in the computed temperature contours, which are shown in Fig. 9. Note that only the right half of the model is shown. The slice in the x-y direction is through the center of the inner fuel injector, as is the first y-z slice. It is clear that only the outer fuel jet ignites, and because of the compressibility effect, does not spread to the center of the model.

Figure 10 shows the computed turbulent Prandtl and Schmidt number contours. As observed in the preceding case, the Prandtl number reaches the floor value in the combustion region. In the fuel jet that does not ignite the Prandtl number is initially low, which results in increased heat conduction to the wall, and then recovers to approximately 1.0 by the exit of the nozzle. The Schmidt number shows somewhat similar trends, varying from the floor value of 0.2 to the maximum of 1.0.

The computations of [15] are compared with the current results and the experimental measurements in Fig. 11. The two simulations are well matched through approximately $x = 0.3$ m. The computation from [15] uses a Pr_t of 0.9 and a Sc_t of 0.5. The constant Pr_t/Sc_t

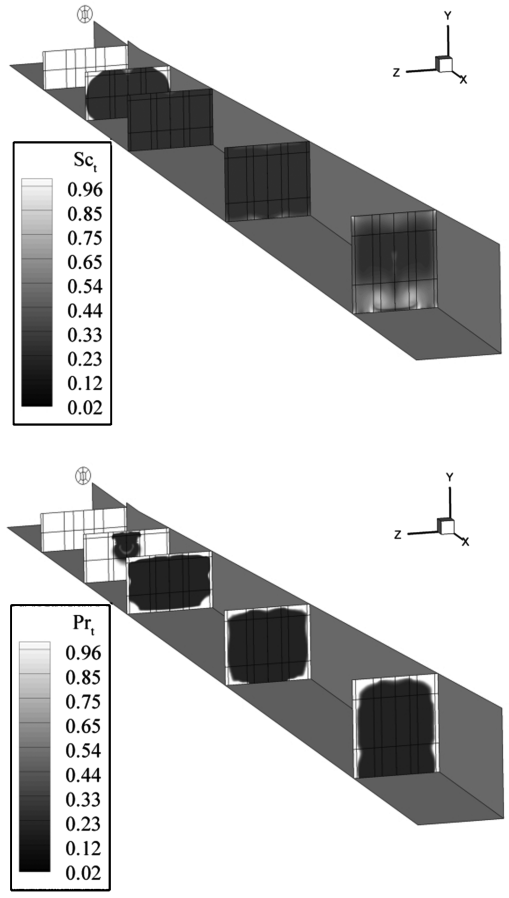

Fig. 7 Computed data only: turbulent Schmidt number (top), and Prandtl number (bottom).

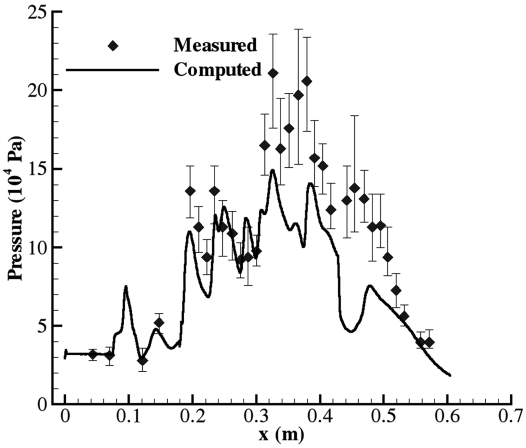

Fig. 8 Computed and measured pressure distribution along center of bottom wall for HyShot case.

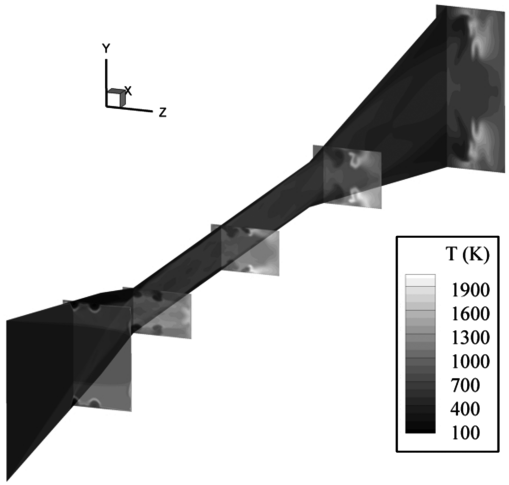

Fig. 9 Computed temperature contours for HyShot case.

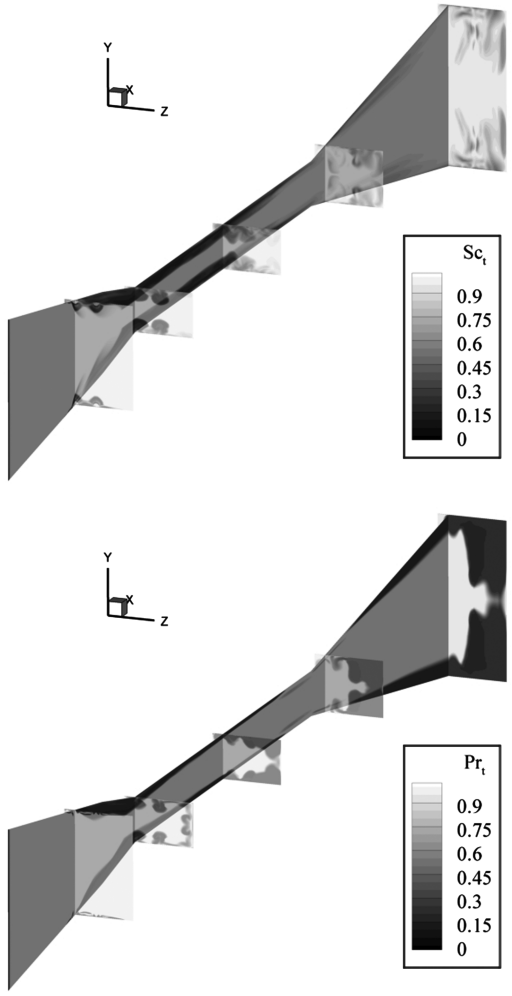

Fig. 10 Contours for HyShot case: computed turbulent Schmidt number (top), and Prandtl number (bottom).

model matches the experimental values slightly further through the combustor but over predicts the pressure near the exit of the combustor. To visualize the flow field inside the combustor, the magnitude of the pressure gradient on the *x*-*y* center plane is plotted in Fig. 12 for both computations. Note that the shock reflections persist much further for the present model. This is likely due to the lower level of mixing and/or combustion.

The current calculations indicate that premixing a significant fraction of fuel with air before reaching the combustor entrance, as

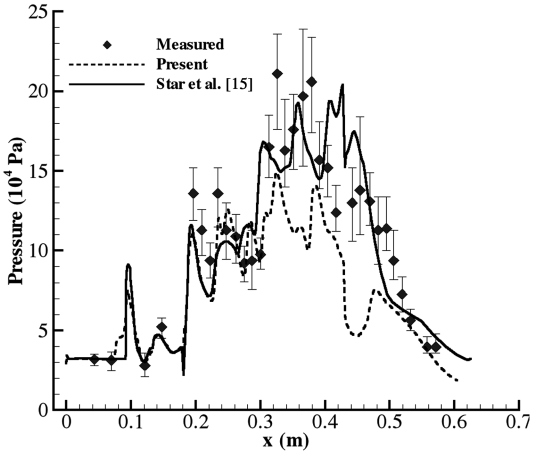

Fig. 11 Comparison of present model with preceding constant Pr_t/Sc_t model simulation of HyShot case.

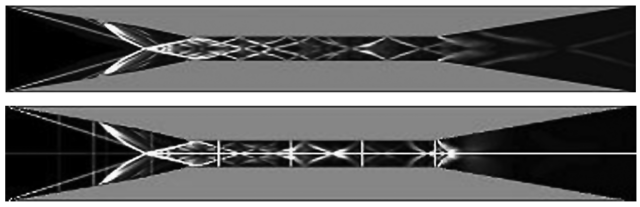

Fig. 12 Pressure gradient magnitude simulation of HyShot case: present model (top) and Star et al. [15] (bottom).

suggested by the radical-farm hypothesis, did not fully materialize. However, the fact that the fuel delivery method resulted in combustion lends some support to the concept.

IV. Conclusions

The current model removes uncertainties resulting from specifying the turbulent Prandtl and Schmidt numbers and ignoring turbulence/chemistry interaction. Moreover, it accounts for compressibility effects.

The model is applied to two distinct 3-D experiments conducted in different facilities. The only common feature is that both use hydrogen as a fuel. Comparisons are made with available measurements of pressure, temperature, and composition. In general, fair to good agreement is indicated. Further improvement of the model will await the availability of well documented experiments that use nonintrusive measurements.

Acknowledgments

This work is funded by the Test and Evaluation/Science and Technology Program through the High Speed/Hypersonic Test focus area managed by Arnold Engineering Development Center (U.S. Air Force), Arnold Air Force Base, Tennessee. The authors would like to thank the Test Resource Management Center Test and Evaluation/ Science and Technology Program for their support.

References

[1] Baurle, R. A., and Eklund, D. R., "Analysis of Dual-Mode Hydrocarbon Scramjet Operation at Mach 4–6.5," *Journal of Propulsion and Power*, Vol. 18, No. 5, 2002, pp. 990–1002. doi:10.2514/2.6047

[2] Robinson, D. F., and Hassan, H. A., "Further Development of the *k*-ζ (Enstrophy) Turbulence Closure Model," *AIAA Journal*, Vol. 36, No. 10, 1998, pp. 1825–1833. doi:10.2514/2.298

[3] Alexopoulos, G. A., "A *k*-ζ (Enstrophy) Compressible Turbulence Model for Mixing Layers and Wall Bounded Flows," *AIAA Journal*, Vol. 35, No. 7, 1997, pp. 1221–1224. doi:10.2514/2.219

[4] Samimy, M., and Elliot, G. S., "Effect of Compressibility on Characteristics of Free Shear Layers," *AIAA Journal*, Vol. 28, No. 3, 1990, pp. 439–445. doi:10.2514/3.10412

[5] Elliot, G. S., and Samimy, M., "Compressible Effects in Free Shear Layers," *Physics of Fluids A*, Vol. 2, No. 7, 1990, pp. 1231–1240. doi:10.1063/1.857816

[6] Goebel, S. G., and Dutton, J. C., "Experimental Study of Compressible Turbulent Mixing Layers," *AIAA Journal*, Vol. 29, No. 4, 1991, pp. 538–546. doi:10.2514/3.10617

[7] Baurle, R. A., Hsu, A. T., and Hassan, H. A., "Assumed and Evolution Probability Density Functions in Supersonic Turbulent Combustion Calculations," *Journal of Propulsion and Power*, Vol. 11, No. 6, 1995, pp. 1132–1138. doi:10.2514/3.23951

[8] Xiao, X., Hassan, H. A., and Baurle, R. A., "Modeling Scramjet Flows with Variable Turbulent Prandtl and Schmidt Numbers," *AIAA Journal*, Vol. 45, No. 6, 2007, pp. 1415–1423. doi:10.2514/1.26382

[9] Cutler, A. D., Danehy, P. M., Springer, R. R., O'Byrne, S., Capriotti, D. P., and DeLoach, R., "Coherent Anti-Stokes Raman Spectroscopic Thermometry in a Supersonic Combustor," *AIAA*

Journal, Vol. 41, No. 12, Dec. 2003, pp. 2451–2459.
doi:10.2514/2.6844

[10] O'Byrne, S., Danehy, P. M., and Cutler, A. D., "Dual-Pump CARS Thermometry and Species Measurements in a Supersonic Combustor," AIAA Paper 2004-0710, Jan. 2004.

[11] White, J. A., and Morrison, J. M., "A Pseudo-Temporal Multi-Grid Relaxation Scheme for Solving the Parabolized Navier–Stokes Equations," AIAA Paper 1999-3360, June 1999.

[12] Rodriguez, C. G., and Cutler, A. D., "CFD Analysis of the SCHOLAR Scramjet Model," AIAA Paper 2003-7039, Dec. 2003.

[13] Rodriguez, C. G., and Cutler, A. D., "Computational Simulation of Supersonic-Combustion Benchmark Experiment," AIAA Paper 2005-4424, July 2005.

[14] Odam, J., and Paull, A., "Internal Combustor Scramjet Pressure Measurements in the T4 Shock Tunnel," AIAA Paper 2002-5244, 2002.

[15] Star, J. B., Edwards, J. R., Smart, M. K., and Baurle, R. A., "Numerical Simulation of Scramjet Combustion in a Shock Tunnel," AIAA Paper 2005-328, Jan. 2005.

[16] Mattick, S., Brinckman, K. W., Dash, S. M., and Liu, Z., "Improvements in Analyzing High-Speed Fuel/Air Mixing Problems Using Scalar Fluctuation Modeling," AIAA Paper 2008-0768, Jan. 2008.

[17] Tomioka, S., Hiraiwa, T., Kobayashi, K., Izumikawa, M., Kishida, T., and Yomashi, H., "Variation Effects on Scramjet Performance in Mach 6 Flight Conditions," *Journal of Propulsion and Power*, Vol. 23, No. 4, 2007, pp. 789–796.
doi:10.2514/1.28149

[18] Lee, S-H., "Characteristics of Dual Transverse Injection in Scramjet Combustor, Part 1: Mixing," *Journal of Propulsion and Power*, Vol. 22, No. 5, 2006, pp. 1012–1019.
doi:10.2514/1.14180

[19] Lee, S-H., "Characteristics of Dual Transverse Injection in Scramjet Combustor, Part 2: Combustion," *Journal of Propulsion and Power*, Vol. 22, No. 5, 2006, pp. 1020–1026.
doi:10.2514/1.14185

[20] Alexander, D. C., and Sislian, J. P., "Computational Study of the Propulsive Characteristics of a Schramjet Engine," *Journal of Propulsion and Power*, Vol. 24, No. 1, 2008, pp. 34-44.
doi:10.2514/1.29951.

[21] McGuire, J. R., Boyle, R. R., and Mudford, N. R., "Radical-Farm Ignition Process in Two-Dimensional Supersonic Combustion," *Journal of Propulsion and Power*, Vol. 24, No. 6, 2008, pp. 1248–1257.
doi:10.2514/1.35562

[22] Keistler, P. G., Xiao, X., Hassan, H. A., and Rodriguez, C. E., "Simulation of Supersonic Combustion Using Variable Turbulent Prandtl/Schmidt Number Formulation," AIAA Paper 2006-3733, June 2006.

[23] Keistler, P. G., Xiao, X., Hassan, H. A., and Cutler, A. D., "Simulation of the SCHOLAR Supersonic Combustion Experiments," AIAA Paper 2007-0835, Jan. 2007.

[24] Keistler, P. G., Hassan, H. A., and Xiao, X., "Role of Chemistry/Turbulence Interaction in 3-D Supersonic Combustion," AIAA Paper 2008-0089, Jan. 2009.

[25] Edwards, J. R., "Advanced Implicit Algorithm for Hydrogen-Air Combustion Calculation," AIAA Paper 1996-3129, June 1996.

[26] Edwards, J. R., "A Low Diffusion Flux Splitting Scheme for Navier–Stokes Calculation," *Computers and Fluids*, Vol. 26, No. 6, 1997, pp. 635–659.
doi:10.1016/S0045-7930(97)00014-5

[27] Jachimowski, C. J., "An Analytic Study of the Hydrogen-Air Reaction Mechanism with Application to Scramjet Combustion," NASA, Report 2791, Feb. 1988.

[28] Conaire, M. O., Curran, H. J., Simmie, J. M., Pitz, W. J., and Westbrook, C. K., "A Comprehensive Modeling Study of Hydrogen Oxidation," *International Journal of Chemical Kinetics*, Vol. 36, No. 11, 2004, pp. 603–622.
doi:10.1002/kin.20036

J. Oefelein
Associate Editor